Structural and Optoelectronic Properties of SnO_2 Nanowires

Jong-Soo Lee, Sung-Kyu Sim , Byung-Don Min, Kyoung-Ah Cho, and Sang-Sig Kim[a]
Department of Electrical Engineering, Korea University, Anam-dong 5-ga, Seongbuk-gu, Seoul 136-701, Korea

[a]E-mail : sangsig@korea.ac.kr

(Received February 27 2004, Accepted April 12 2004)

Structural and optoelectronic properties of as-synthesized SnO_2 nanowires were examined in this study. The SnO_2 nanowires were first synthesized by thermal evaporation of ball-milled SnO_2 powders in argon atmosphere without the presence of any catalysts, and their structural properties are then investigated by X-ray diffraction, Raman scattering, scanning electron microscopy, and transmission electron microscopy. This investigation revealed that the synthesized SnO_2 nanowires are single-crystalline and that their growth direction is parallel to the [100] direction. In addition, photoresponse of a single SnO_2 nanowire was performed with light with above-gap energy, and different characteristics of photoresponses were obtained for the nanowire at ambient atmosphere and in vacuum. The photoresponse mechanism is briefly discussed in this paper.

Keywords : SnO_2 nanowire, Photoresponse, TEM

1. INTRODUCTION

Wide-bandgap SnO_2 semiconducting material (E_g = 3.6 eV at room temperature) is one of the attractive candidates for optoelectronic devices operating at room temperature, gas sensors, and transparent conducting electrodes[1,2]. The synthesis and gas sensing properties of semiconducting SnO_2 nanomaterials have became one of important research issues since the first synthesis of SnO_2 nanobelts by Wang group[3]. Recently, a considerable number of studies have been reported on the synthesis of SnO_2 nanomaterials (nanowires, nanorods, and nanobelts etc.) using laser ablation[4], thermal decomposition[5], thermal evaporation[6,7], rapid oxidation[8], and redox reaction[9], yet there are a few reports on the gas sensing and optoelectronic properties of SnO_2 nanowires. In this study, SnO_2 nanowires were first grown on a Si (100) substrate from thermal evaporation of ball-milled SnO_2 powders without the presence of any catalysts. The structural and optoelectronic properties of the as-synthesized SnO_2 nanowires are then examined by X-ray diffraction (XRD), field emission scanning electron microscopy (FE-SEM), transmission electron microscopy (TEM), Raman scattering, and photoresponse. In addition, the photoresponse mechanism is briefly discussed in this paper.

2. EXPERIMENTAL PROCEDURE

SnO_2 powders were used for synthesizing nanowires under study. The starting SnO_2 powders were first ground for 20 hours in a mechanical ball mill system using a steel vial with 100 stainless steel balls in which the mixture ratio of steel balls and the SnO_2 powders was 15:1 in weight percents. An alumina boat containing the ball-milled SnO_2 powders was then loaded into the center of a horizontal alumina tube and a 5×5mm-sized silicon substrate was put at the downstream end of the alumina tube. The thermal evaporation of the ball-milled SnO_2 powders was performed at 1380 ℃ for 2 hours with an argon flow rate of 500 standard cubic centimeters per minute (sccm). The as-synthesized products were characterized by XRD (RIGAKU, D/MAX-□A) with CuKα (λ=1.54184 Å) radiation, FE-SEM (HITACHI, S-4700), TEM (JEOL, JEM-2010) for the analysis of their nanostructure. For the optoelectronic studies, Ti/Au metals were deposited onto a degenerately doped silicon wafer covered with a 100-nm thick Al_2O_3 film for the preparation of electrodes. After the sonication of the SnO_2 nanowires for 20 seconds in methanol, these nanowires were dispersed onto two Ti/Au electrodes. Photocurrent measurement was made for a single SnO_2 nanowire in air or in vacuum at 300 K. The light source for this measurement was the 325 nm-wavelength line from a He-Cd laser; the power density of the light was 10 mW/cm^2.

3. RESULTS AND DISCUSSION

Figure 1 shows the SEM image (a) of SnO_2 nanowires synthesized from the thermal evaporation of the ball-milled SnO_2 powders and the distribution (b) of the diameters of these nanowires. Our SEM analysis was performed over fifty nanowires to obtain the distribution shown in Fig. 1(b). The SnO_2 nanowires are in the range of 10 to 120 nm in diameter, and the mean diameter obtained from the distribution is about 40 nm. And their length ranges from 10 to 70 μm.

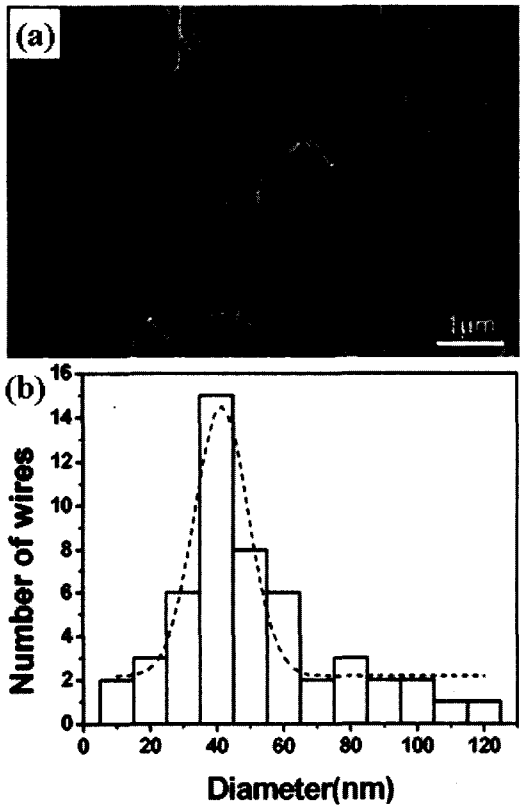

Fig. 1. SEM image (a) and diameter distribution (b) of as-synthesized SnO_2 nanowires.

Figure 2 shows the XRD patterns of the starting SnO_2 powders and the as-synthesized SnO_2 nanowires (a) and their magnified patterns (b). The XRD pattern of the SnO_2 powders is indexed to the tetragonal rutile structure with lattice constants of a=0.473 nm and c=0.318 nm from JCPDS card (41-1444). The representative XRD pattern of the SnO_2 nanowires is identical to that of the SnO_2 powders, indicating that these nanowires are indeed SnO_2. In addition, a careful comparison between the magnified XRD patterns in Fig. 2(b) reveals that three XRD peaks for the SnO_2 nanowires are shifted to the lower diffraction angle, as compared with the SnO_2 powders; the shift is $\Delta(2\theta)$ = 0.09, 0.1, and 0.06 degrees for the (110), (101), and (200) peaks, respectively. This shift of the XRD peaks toward the lower Bragg angle means the larger distances between the neighboring lattice planes for the SnO_2 nanowires than those for the SnO_2 powders. This observation indicates that the SnO_2 nanowires experience tensile stress, compared with the SnO_2 powders.

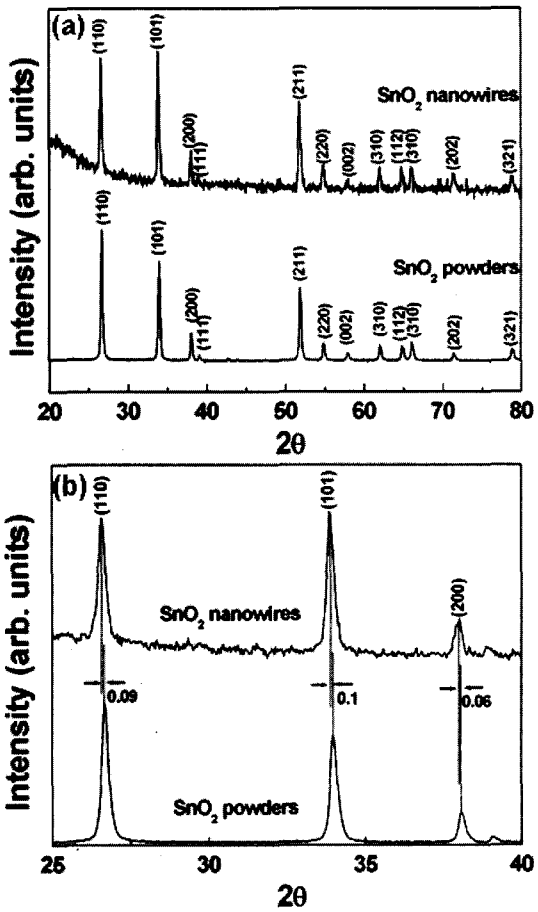

Fig. 2. XRD patterns of SnO_2 powders and as-synthesized SnO_2 nanowires (a) and their magnified patterns (b).

Figure 3 shows the room-temperature Raman scattering spectra of the starting SnO_2 powders and the SnO_2 nanowires, respectively. The Raman peaks of the starting SnO_2 powders are detected at 474, 636, and 776 cm^{-1}, corresponding to the E_g, A_{1g}, and B_{2g} vibration modes of rutile bulk SnO_2, respectively [5,6,10]. For the SnO_2 nanowires, the Raman peaks are down-shifted, compared with the SnO_2 powders; the E_g, A_{1g}, and B_{2g} vibration modes are present at 473, 634, and 767 cm^{-1}, respectively. This shift is more associated with the size effect rather than the stress effect; a small dimension of the nanowires leads to a downshift of the Raman peaks [11], and for the nanowires under tensile stress Raman peaks are shifted toward higher frequency region[12].

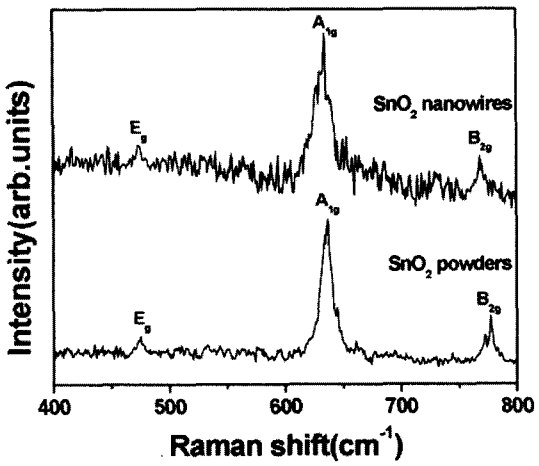

Fig. 3. Raman spectra of as-synthesized SnO_2 nanowires and SnO_2 powders.

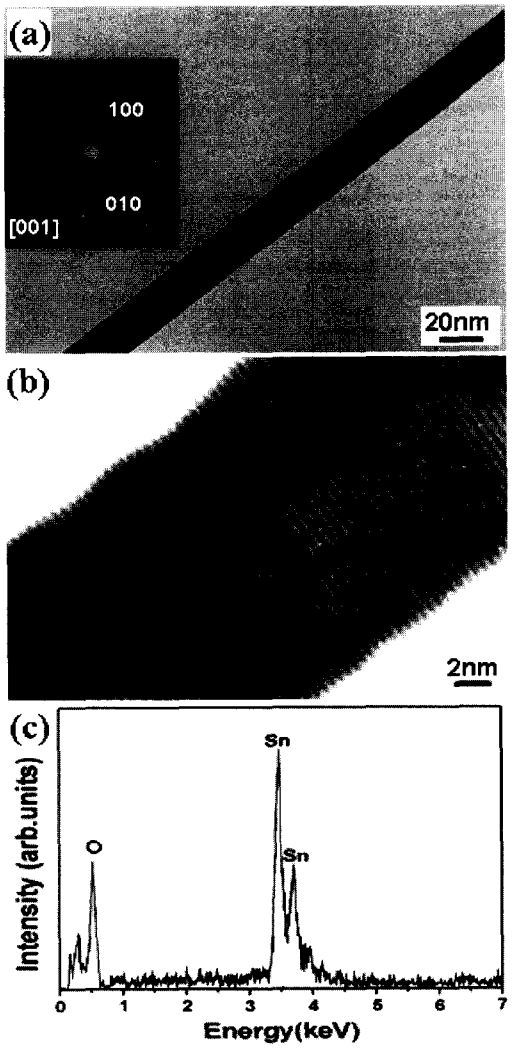

Fig. 4. TEM (a) and HRTEM (b) images of a selected SnO_2 nanowire, and its associated EDX spectrum (c); its SAED pattern is given in the inset.

Figure 4 shows the TEM (a) and the high-resolution TEM (HRTEM) images (b) of a selected SnO_2 nanowire, and its associated EDX spectrum (c). The TEM image of Fig. 4(a) shows the straight-line morphology with a diameter of about 20nm. The inset of Fig. 4(a) shows a representative selected-area electron diffraction (SAED) pattern taken from this SnO_2 nanowire. In the SAED pattern, the direction of the zone axis is indexed to be the [001] direction for the nanowire. The SAED pattern demonstrates the single-crystalline spots and the growth direction parallel to the [100] direction. The HRTEM image of Fig. 4(b) shows that the nanowire is structurally uniform, and its clear lattice fringe illustrates that the nanowire is single-crystalline, and dislocation and point defects free.

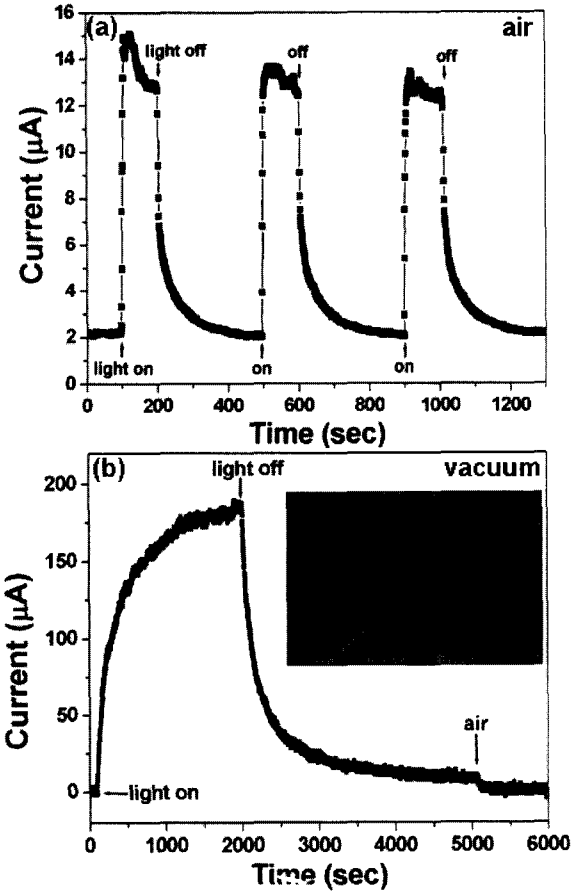

Fig. 5. Photoresponse of a single SnO_2 nanowire in air (a) and in vacuum (b) at a bias voltage of 1.0 V; the inset shows the single SnO_2 nanowire lying two electrodes.

The interplanar spacing of the selected nanowire is about 0.47 nm, corresponding to the distance of the neighboring (100) planes in tetragonal rutile SnO_2 structure. In the EDX spectrum depicted in Fig. 4(c), only peaks associated with Sn and O elements are present and

any other Fe- or Cr-related peaks are absent. The ball-milled SnO_2 powders were significantly contaminated by Fe and Cr metal particles coming from stainless steel balls while milling, yet the EDX spectrum reveals that the relatively purified SnO_2 nanowires were synthesized from the contaminated SnO_2 powders.

Figure 5 shows the photoresponse of a single SnO_2 nanowire in air (a) and in vacuum (b) at a bias voltage of 1.0 V; the inset of Fig. 5(b) shows the single nanowire lying on two electrodes. For the single nanowire in air (Fig. 5(a)), the photocurrent was increased rapidly when the 325 nm-wavelength light was switched on, and it was saturated. After the light was switched off, the current was decayed to about one hundredth of the saturated value within 100~300 seconds. In contrast, for the single nanowire in vacuum (Fig. 5(b)), the photocurrent was gradually increased in 2000 seconds without the saturation under the illumination of the light to a value larger than the saturated one in air by 150 times in magnitude. After the light was turned off, the current was decreased slowly, compared with the nanowire in air. When the air was introduced, the current was decreased rapidly.

It has been well-known that the photoresponse of n-type oxide semiconductors is controlled by surface effects such as oxygen adsorption under dark conditions by trapping electrons ($O_2(g)+e^- \rightarrow O_2^-(ad)$) and photo-desorption of oxygen ions by capturing photogenerated holes ($h^+ + O_2^-(ad) \rightarrow O_2(g)$)[13, 14]. The adsorption and photodesorption mechanism may be applicable to the SnO_2 nanowire under study. On the basis of the established photocurrent mechanism of n-type oxide semiconductors, the observed photoresponse of the SnO_2 nanowire may be explained. For the SnO_2 nanowire in air, negatively charged oxygen ions are detached from their surface by capturing holes generated under the illumination, leading to a thinning of the depletion layer near their surface. The thinning of the depletion layer allows more number of electrons to transport inside the nanowire, causing the rise of the photocurrent. The saturated photocurrent observed in the nanowire in air under the illumination originates from the equilibrium that the number of the oxygen ions adsorbed on the surface from air is the same as the number of the photodesorbed oxygen ions escaped from the surface to air. For the nanowire in vacuum under the illumination, the photocurrent increases without saturation since the depletion layer narrows continuously due to the continuous photodesorption of oxygen ions. When oxygen is introduced to the nanowire initially in vacuum in dark, the current is decayed more rapidly due to the extension of the depletion layer caused by the introduction of the negatively charged oxygen ions than the nanowire in vacuum in dark.

4. CONCLUSION

SnO_2 nanowires synthesized from the ball-milled SnO_2 powders without the presence of any catalysts are in the range of 10 to 120 nm in diameter and in the range of 10 to 70 μm in length. These synthesized SnO_2 nanowires are single-crystalline and their growth direction is parallel to the [100] direction. Our XRD study indicates that the SnO_2 nanowires experience tensile stress, compared with the SnO_2 powders, yet the shift of the Raman scattering peaks to lower frequency is more associated with the size effect rather than the stress effect. For the single nanowire in air, the photocurrent was increased rapidly under the illumination, and it was saturated. In contrast, for the single nanowire in vacuum, the photocurrent was increased without the saturation under the illumination of the light. The observed photoresponse of the SnO_2 nanowire may be explained on the basis of the established photocurrent mechanism of n-type oxide semiconductors.

ACKNOWLEDGES

This work was supported by the Korean Ministry of Science and Technology as a part of the '03 Nuclear R&D Program, Grant No. M2-0363-00-0052, Grant No. R01-1999-000-00230-0, Grant No. R01-2002-000-00504 -0 from the Basic Research Program of the Korea Science & Engineering Foundation, Korea University Grant and National R&D project for Nano Science and Technology.

REFERENCES

[1] G. Ansari, P. Boroojerdian, S. R. Sainkar, R. N. Karekar, R. C. Alyer, and S. K. Kulkarni, "Grain size effects on H_2 gas sensitivity of thick film resistor using SnO_2 nanoparticles", Thin Solid Films, Vol. 295, p. 271, 1997.

[2] Y. S. He, J. C. Campbell, R. C. Murphy, M. F. Arendt, and J. S. Swinnea, "Electrical and optical characterization of Sb : SnO_2", J. Mater. Res., Vol. 8 , p. 3131, 1993.

[3] Z. W. Pan, Z. R. Dai, and Z. L. Wang, "Nanobelts of Semiconducting Oxides", Science, Vol. 291, p. 1947, 2001.

[4] J. Hu, Y. Bando, and Q. Liu, D. Golberg, "Laser-ablation growth and optical properties of wide and long single-crystal SnO_2 ribbons", Adv. Funti. Mater., Vol. 13, p. 493, 2003.

[5] C. Xu, G. Xu, Y. Liu, X. Zhao, and G. Wang, "Preparation and characterization of SnO_2 nanorods by thermal decomposition of SnC_2O_4 precursor",

Scripta Materialia, Vol. 46, p. 789, 2002.
[6] Z. R. Dai, J. L. Gole, J. D. Stout, and Z. L. Wang, "Tin oxide nanowires, nanoribbons, and nanotubes", J. Phys. Chem. B, Vol. 106, p. 1274, 2002.
[7] S. H. Sun, G. W. Meng, G. X. Zhang, T. Gao, B. Y. Geng, L. D. Zhang, and J. Zuo, "Raman scattering study of rutile SnO_2 nanobelts synthesized by thermal evaporation of Sn powders", Chem. Phys. Lett., Vol. 376, p. 103, 2003.
[8] X. L. Ma, Y. Li, and Y. L. Zhu, "Growth mode of the SnO_2 nanobelts synthesized by rapid oxidation", Chem. Phys. Lett., Vol. 376, p. 794, 2003.
[9] Y. Liu, C. Zheng, W. Wang, Y. Zhan, and G. Wang, "Production of SnO_2 nanorods by redox reaction", J. Cryst. Growth, Vol. 233, p. 8, 2001.
[10] K. N. Yu, Y. H. Xiong, Y. L. Liu, and C. S. Xiong, "Microstructure change of nano-SnO_2 grain assemblages with the annealing temperature", Phys. Rev. B, Vol. 55, p. 2666, 1997.
[11] I. H. Campbell and P. M. Fauchet, "The effects of microcrystal size and shape on the one phonon Raman spectra of crystalline semiconductors", Solid State Commun., Vol. 58, p. 739, 1986.
[12] H. W. Seo, S. Y. Bae, J. Park, H. Yang, K. S. Park, and S. Kim, "Strained gallium nitride nanowires", J. Chem. Phys., Vol. 116, p. 9492, 2002.
[13] D. A. Popescu, J. M. Herrmann, A. Ensuque, and F. Bozon-Verduraz, "Nanosized tin dioxide: Spectroscopic (UV-VIS, NIR, EPR) and electrical conductivity studies", Phys. Chem. Chem. Phys., Vol. 3, p. 2522, 2001.
[14] J. H. Ding, T. J. McAvoy, R. E. Cavicchi, and S. Semancik, "Surface state trapping models for SnO_2-based microhotplate sensors", Sens. Actuators B, Vol. 77, p. 597, 2001.